

NOTE • OPEN ACCESS


MR-OCTAVIUS 4D with 1500 MR and 1600 MR arrays is suitable for plan QA in a 1.5 T MRI-linac

To cite this article: Viktoriia Gorobets *et al* 2024 *Phys. Med. Biol.* **69** 17NT01


View the [article online](#) for updates and enhancements.

You may also like

- [Hierarchical multi-level dynamic hyperparameter deformable image registration with convolutional neural network](#)
Zhenyu Zhu, Qianqian Li, Ying Wei et al.
- [CT-based synthetic contrast-enhanced dual-energy CT generation using conditional denoising diffusion probabilistic model](#)
Yuan Gao, Richard L J Qiu, Huiqiao Xie et al.
- [Pre-clinical evaluation of dual-layer spectral computed tomography-based stopping power prediction for particle therapy planning at the Heidelberg Ion Beam Therapy Center](#)
Friderike K Faller, Stewart Mein, Benjamin Ackermann et al.



Joining forces:
One complete
QA solution for
Dosimetry with
myQA[®], QUASAR[™]
and Radcal[®]!





NOTE

MR-OCTAVIUS 4D with 1500 MR and 1600 MR arrays is suitable for plan QA in a 1.5 T MRI-linac

OPEN ACCESS

RECEIVED
12 April 2024REVISED
11 July 2024ACCEPTED FOR PUBLICATION
25 July 2024PUBLISHED
14 August 2024Viktoriia Gorobets¹ , Wilfred de Vries², Nicole Brand², Thomas Foppen¹, André J M Wopereis¹ and Simon Woodings^{1,*}¹ University Medical Center Utrecht, The Netherlands² PTW Freiburg, Germany

* Author to whom any correspondence should be addressed.

E-mail: jwooding@umcutrecht.nl**Keywords:** OCTAVIUS Detector 1500 MR, OCTAVIUS Detector 1600 MR, OCTAVIUS 4D Phantom MR, MR-Linac, patient specific quality assuranceOriginal Content from
this work may be used
under the terms of the
[Creative Commons
Attribution 4.0 licence](https://creativecommons.org/licenses/by/4.0/).Any further distribution
of this work must
maintain attribution to
the author(s) and the title
of the work, journal
citation and DOI.**Abstract**

To ensure the accuracy of radiation delivery to patients in a 1.5 T MRI-linac, the implementation of quality assurance (QA) devices compatible with MR technology is essential. The OCTAVIUS 4D MR, made by PTW (Freiburg, Germany) is designed to ensure consistent and ideal alignment of its detectors with the direction of each beam segment. This study focuses on investigating the fundamental characteristics of the detector response for the OCTAVIUS Detector (OD) 1500 MR and OCTAVIUS 1600 MR when used in the MR-compatible OCTAVIUS 4D. Characteristics examined included short-term reproducibility, dose linearity, field size dependency, monitor unit (MU) rate dependency, dose-per-pulse dependency, and angular dependency. The evaluation of OD 1500 MR also involved measuring 25 clinical treatment plans across diverse target sizes and anatomical sites, including the liver/pancreas, rectum, prostate, lungs, and lymph nodes. One plan was measured with the standard setup and with a 5 cm left offset. The OD 1600 MR was not available for these measurements. The capability of the OD 1500 MR to identify potential errors was assessed by introducing a MU and positional shift within the software. The results demonstrated no significant differences in short-term reproducibility (<0.2%), dose linearity (<1%), field size dependency (<0.7% for field sizes larger than 5 cm × 5 cm), MU rate dependency (<0.8%), dose-per-pulse dependency (<0.4%) and angular dependency (standard deviation <0.5%). All tests of clinical plans were successfully completed. The OD 1500 MR demonstrated compatibility with the standard 95% pass rate when employing a global 3%/3 mm gamma criterion, and a 90% pass rate using a global 2%/2 mm gamma criterion. The detector demonstrated the capacity to measure treatment plans with a 5 cm left offset. With the standard parameters, the gamma test was sensitive to position errors but required an addition tests of mean/median dose or point dose in order to detect small dose difference.

1. Introduction

The Elekta Unity MRI-Linac (MRL) integrates a 7 MV linear accelerator (linac) with a 1.5 T MR-scanner (Philips Medical Systems, The Netherlands), enabling simultaneous irradiation and high-quality imaging. This combination enhances the contrast and visualization of soft tissue in the target area (Lagendijk *et al* 2014).

Before initiating patient therapy, it is crucial to conduct comprehensive quality assurance (QA) of the treatment plans to ensure accurate delivery of the intended dose distributions (Ezzell *et al* 2003). However, the presence of a 1.5 T transverse magnetic field in the MR-Linac affects dose deposition and can potentially impact the accuracy of the dosimetry equipment (Houweling *et al* 2016).

2D ion chamber detector arrays are now commonly used in many hospitals for linac QA. These devices are distinguished by the size of each detector, the specific type and arrangement of these detectors, and the number of detectors within the measurement area (Stelljes *et al* 2015). These arrays have their limitations. First of all, the detection volume is limited by the minimum size needed to produce a sufficient signal (Pappas *et al* 2006, Stelljes *et al* 2015). Readings are affected by signal averaging over the sensitive volume and secondary electron transport across its wall (Ezzell *et al* 2003, Laub and Wong 2003). Liquid-filled ionization chambers enable the reduction of the sensitive volume due to the higher density of the liquid compared to air. However, this results in increased initial ion recombination (Pardo-Montero and Gómez 2009). Such deviations caused by both volume averaging effect and ion recombination have been previously reported for small field sizes (Poppe *et al* 2006, Van Esch *et al* 2014, Stelljes *et al* 2015).

Detectors from PTW (Freiburg, Germany) such as OCTAVIUS 2D ionization chamber arrays (1500 and 1600 SRS) and various phantoms (Octagonal and 4D) for patient plan-specific QA has been well-established in 0 T conventional systems (Poppe *et al* 2006, Van Esch *et al* 2014, Stelljes *et al* 2015, Olaciregui-Ruiz *et al* 2019, Brand *et al* 2022). A significant angular sensitivity around 90° has been observed when using an octagonal phantom (Van Esch *et al* 2014).

MR-compatible detector arrays, such as the OD 1500 MR with air-filled ion chambers and the OD 1600 MR with liquid-filled ion chambers, have been evaluated in magnetic fields (0.35 T and 1.5 T) using the older non-rotating phantom. These tests have also revealed considerable angular sensitivity with a 20% gamma percentage difference reduction (Mönnich *et al* 2020, Poppinga *et al* 2021).

PTW is introducing the MR-compatible OCTAVIUS 4D system, which is specifically designed to rotate, ensuring a constant and optimal alignment between detectors and each beam segment direction. This characteristic is especially important in treatment settings that use MRI technology. The fully MR-compatible system is now available for testing and implementation in MR-Linacs.

The purpose of this study is to evaluate the suitability of the MR-compatible system for patient plan QA in a 1.5 T MR-linac. Fundamental dosimetry tests were conducted on the OD 1500 MR and OD 1600 MR within the OCTAVIUS 4D Phantom MR. Additionally, 25 patient treatment plans were evaluated using OD 1500 MR and OCTAVIUS 4D MR. One lung plan with high dose region offset was measured when the position of the OCTAVIUS 4D MR was shifted 5 cm to the left.

2. Materials and methods

The study's measurements were conducted using the OD 1500 MR and OD 1600 MR arrays (figure 1) along with the OCTAVIUS 4D Phantom MR.

2.1. OCTAVIUS Detector 1500 MR

The OD 1500 MR array consists of 1405 cubic vented ion chambers arranged in a plane-parallel configuration, forming a chessboard matrix pattern on a 27 cm × 27 cm grid. Each individual chamber covers a 4.4 mm × 4.4 mm area with a height of 3 mm, giving it an active volume of approximately 0.06 cm³. The reference point specified by the manufacturer is located 7.5 mm beneath the surface. The array is equipped with an electrometer capable of accommodating a dose rate from 0.25 Gy min⁻¹ up to 96 Gy min⁻¹. The base plate beneath the ion chambers is constructed from a material nearly equivalent to water (polystyrene), and the detector frame is crafted from glass-reinforced plastic. The device's absolute dose calibration is established by the manufacturer using a ⁶⁰Co beam.

2.2. OCTAVIUS Detector 1600 MR

The OD 1600 MR array consists of 1521 cubic liquid-filled ion chambers arranged in a plane-parallel configuration with an active detector area of 15 cm × 15 cm. The reference point is located 9 mm beneath the surface of the array. Each chamber covers a 2.5 mm × 2.5 mm area with a height of 0.5 mm, resulting in an active volume of 0.003 cm³. In the central (6.5 cm × 6.5 cm) area of the array, detectors have a 2.5 mm high-resolution spacing. Outside the central area, the spacing is 5 mm. The associated electrometer can handle a dose rate from 0.1 Gy min⁻¹ up to 24 Gy min⁻¹.

2.3. Basic dosimetric characteristics of the OD 1500 MR and OD 1600 MR arrays

Both detectors underwent fundamental dosimetric characterization. The results were compared to Farmer-type ion chamber measurements. Deviations were calculated from the readings under reference conditions.

The basic dosimetric characteristics of both detectors were measured using a simple setup at 0° gantry angle. The arrays were positioned below a 5 cm buildup cap of RW3 slabs (PTW, Freiburg, Germany) of 30 cm × 30 cm. The Farmer chamber (Type 30013, PTW-Freiburg, Germany) was inserted into the farmer

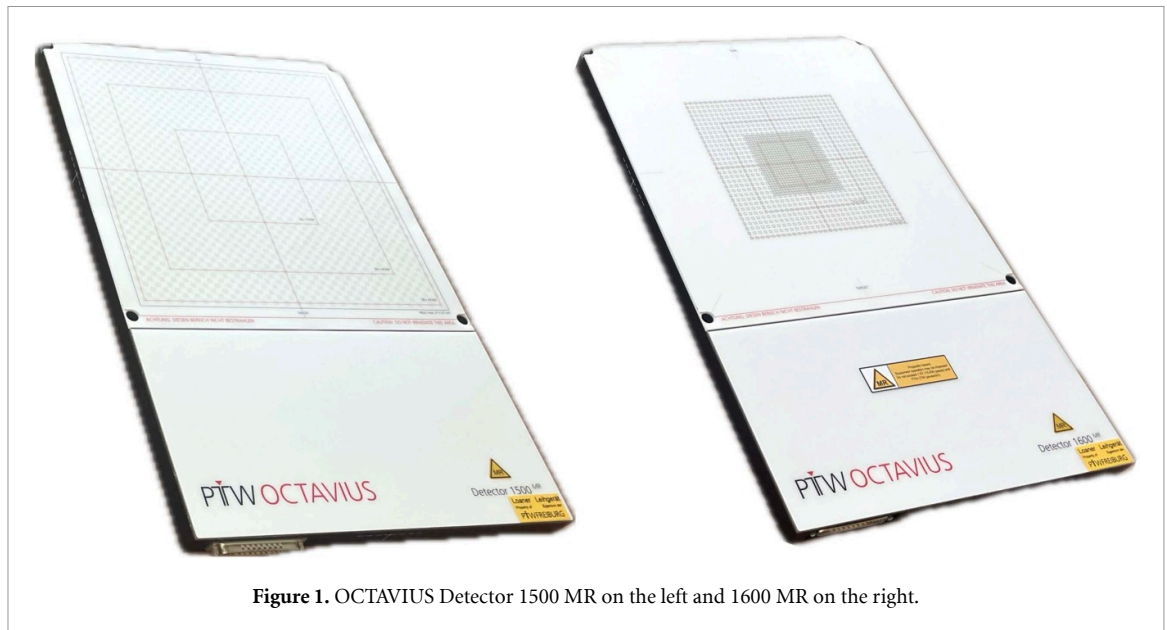


Figure 1. OCTAVIUS Detector 1500 MR on the left and 1600 MR on the right.

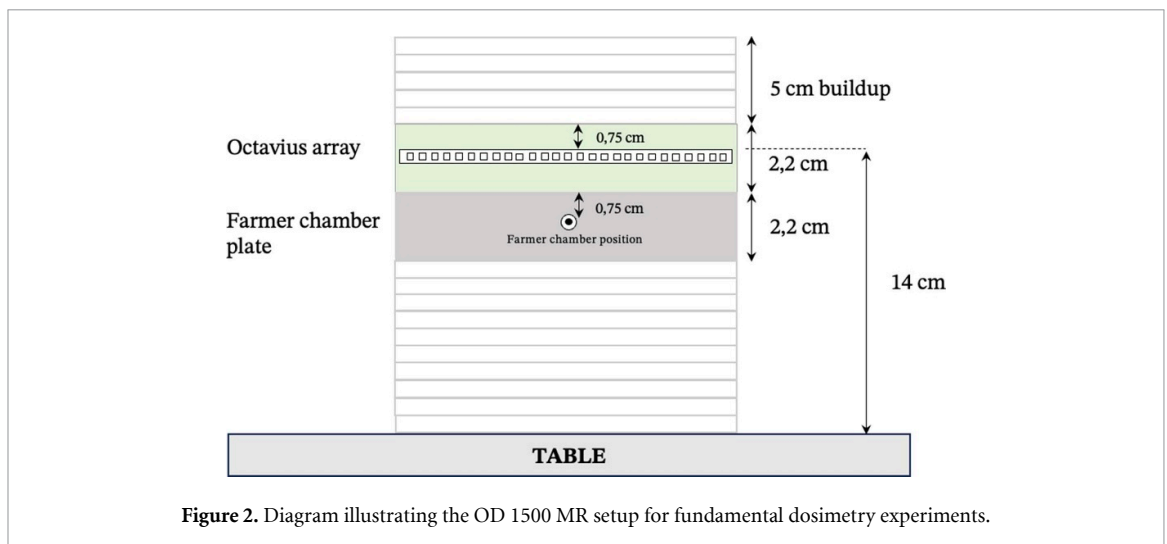


Figure 2. Diagram illustrating the OD 1500 MR setup for fundamental dosimetry experiments.

chamber plate of 2.2 cm height and positioned under the detector plate so that both the central ionization chamber of the OD and Farmer chamber were positioned on beam central axis. The OD was arranged to ensure that its central chamber aligned with the linac isocenter, located 14 cm above the couch (figure 2). The height was achieved using RW3 slabs. Both detectors were positioned in the MRI room overnight before measurements to acclimatize.

The measurements were conducted using a reference field size of $10\text{ cm} \times 10\text{ cm}$, a gantry angle of 0° , 100 monitor units (MU) per measurement, a dose rate of 426 MU min^{-1} , and a source-to-detector distance (SDD) of 143.5 cm. Angular dependency was measured using the cylindrical OCTAVIUS 4D MR. Before conducting the tests, all detectors underwent pre-irradiation with 1000 monitor units and its maximum field size.

2.3.1. Short-term reproducibility

The short-term reproducibility was assessed by performing ten consecutive measurements of the central chamber under reference setup conditions. The standard deviation and maximum deviation were calculated. The results were compared to the mean value obtained from all ten measurements.

2.3.2. Dose linearity

The dose linearity test involved measuring readings for 2–1000 MU. Reference values were obtained using the standard setup with 100 MU. Percentage differences were calculated by comparing measured readings to the reference values acquired with 100 MU.

2.3.3. Dose per pulse dependency

Dose per pulse dependency was measured on the MRL at different Source-to-Detector Distances (SDD). As the table height remains fixed on an MRL, the variations in height were achieved by adjusting the phantom. To achieve the necessary SDDs, we employed 5 cm of buildup along with 5–32 cm of backscatter. Measurements for the Farmer chamber and OCTAVIUS devices were taken separately to maintain the same SDD. The SDDs used for the measurements, defined as the distances from the target to the central chamber, were 125.5 cm, 134.5 cm, 143.5 cm, and 152.5 cm. The corresponding dose per pulse values ranged from 0.23 to 0.35 mGy. To assess the variations, the percentage differences were calculated by comparing these readings to the reference values obtained at 143.5 cm SDD.

2.3.4. MU rate dependency

The MU rate dependency was evaluated by varying the MU rate on the MRL. Dose rates of 25–530 MU min⁻¹ were applied in 8 steps. Percentage differences were then calculated by comparing these readings to the reference values at 426 MU min⁻¹.

2.3.5. Field size dependency

The assessment of field size (FS) dependence for the OD 1500 MR array involved measuring the maximum readings around the central chamber across various field sizes, specifically 1 × 1, 2 × 2, 3 × 3, 5 × 5, 10 × 10, 15 × 15, 20 × 20, 22 × 22, and 22 × 27 cm². The maximum length of the field is limited to 22 cm in the MRL.

In the case of the OD 1600 MR array, the field sizes were 1 × 1, 2 × 2, 3 × 3, 5 × 5, 8 × 8, 10 × 10, 12 × 12, and 15 × 15 cm². Here, the maximum field size is limited by the dimensions of the detector plate.

The minimum field size for both detector arrays is constrained by the dimensions of the individual chambers. PTW recommended minimum field sizes of 2 × 2 cm² for OD 1500 MR and 1 × 1 cm² for OD 1600 MR. In this experiment, the tests were extended to fields smaller than the recommended values.

The reference values were calculated in the Monaco treatment planning system based on PTW microDiamond commissioning data. Percentage differences were then calculated.

2.3.6. Angular dependency

The angular dependence was investigated by varying the gantry angle from 0° to 360° with 10° steps. The phantom was rotated synchronously to the gantry. The central chamber was positioned perpendicular to the incident beam. The measurements for the arrays and the Farmer chamber were conducted separately ensuring that the axis of rotation remained consistent for both. Deviations were then calculated by comparing the readings at different angles to the reference value obtained at 0°.

2.4. Plan QA in the cylindrical OCTAVIUS 4D Phantom MR

25 clinical treatment plans across various target sizes and anatomical sites (liver/pancreas, rectum, prostate, lungs, and lymph nodes) were measured using the OD 1500 MR in the OCTAVIUS 4D MR. The automatic alignment was applied per each plan. The capability of the OCTAVIUS 4D MR to measure doses with an offset was tested by evaluating one lung treatment plan with a high-dose region offset. This was done by positioning the MR-Octavius 4D isocenter 5 cm to the left. Because the 1.5 T magnetic field is highly uniform throughout the array (Roberts 2021), a measurement with the right offset was assumed to show only minor symmetrical differences and was not performed due to the absence of a suitable plan.

For the evaluation, we employed 3D global gamma comparison analysis with a 3%/3 mm and 2%/2 mm criterion (Ezzell 2009, Heilemann *et al* 2013, Miften 2018), using VeriSoft software (Version 8.1). The low dose threshold was set to 10%.

Evaluations were also conducted on plans containing errors using the gamma comparison analysis. Instead of directly measuring error-containing plans, errors were deliberately introduced to the TPS dose distribution in VeriSoft by modifying the number of MU by a margin of -10% to +10% relative to the original plan, or by shifting the isocenter position by 1–5 mm. The initial results without automatic alignment were used for the evaluation.

The ability of the detector to identify plans with deliberate errors was tested by statistically comparing standard plan results to the plans with errors using Wilcoxon signed-rank test. It was hypothesized that the results for plans with errors would be lower than those of the standard plans, and a $p < 0.05$ validated this hypothesis.

Table 1. Maximum deviation (%) and standard deviation (%) for each dosimetry test for OCTAVIUS Detector 1500 MR and 1600 MR. All test results were acceptable for clinical use.

Dosimetry test	OCTAVIUS Detector 1500 MR		OCTAVIUS Detector 1600 MR	
	Max deviation, %	STD, %	Max deviation, %	STD, %
Short-term reproducibility	0.2	0.1	0.1	0.1
Dose linearity	0.4	0.2	0.95	0.3
Dose-per-pulse dependence	0.1	0.1	0.4	0.2
Field dependence	4.0	0.1	0.1	1.6
MU rate dependence	0.3	0.1	0.8	0.4
Angular response	1.0	0.3	1.1	0.5

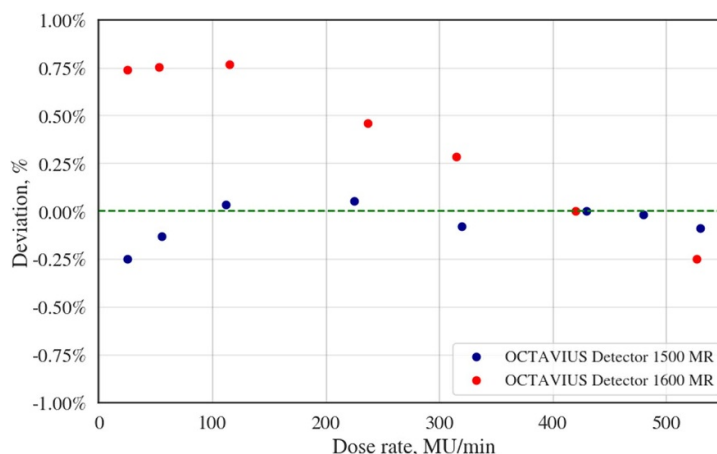


Figure 3. The MU rate dependence of the OD 1500 MR and OD 1600 MR compared to the reference Farmer chamber. The data were normalized to 426 MU min⁻¹. Standard deviations were $\leq 0.4\%$. The OD 1600 MR shows a trend of decreasing sensitivity with an increasing MU rate.

3. Results and discussion

3.1. Basic dosimetric characteristics of the OD 1500 MR and OD 1600 MR arrays

3.1.1. Short-term reproducibility, dose linearity and dose per pulse dependency

The arrays demonstrate consistent short-term reproducibility with maximum deviations of no more than 0.2%. Our findings corroborate the manufacturer's declared reproducibility of $\pm 0.5\%$. In the dose linearity tests, the most significant deviation observed is 0.95% for the 2MU measurement with the OD 1600 MR. Nonetheless, for both devices, all other measurements remain within a deviation range of 0.5%. The dose per pulse dependency of the arrays also remains stable, with maximum deviations of no more than 0.4%. The results of all tests for each detector plate are summarized in table 1.

3.1.2. MU rate dependency

Both detector arrays demonstrate deviations less than 0.8% across a range of MU rates from 30 to 530 MU min⁻¹, which is acceptable for clinical use. Notably, the OD 1600 MR shows a trend of decreasing sensitivity with increasing MU rate (MU min⁻¹), consistent with a previous investigation by PTW. This behavior is attributed to increased recombination with increasing MU rate in the liquid-filled ion chambers (figure 3) (Knill *et al* 2016, Takei *et al* 2018).

3.1.3. Field size dependency

In both medium and large field sizes, both the OD 1500 MR and OD 1600 MR perform well, with deviations of less than 0.7% from the calculations based on commissioning data in the treatment planning system (figure 4). For smaller fields, the OD 1500 MR tends to underestimate the relative output factors (ROFs) due to volume averaging in its 4.4 mm \times 4.4 mm \times 3 mm detectors. Conversely, the OD 1600 MR tends to overestimate the relative output factors ($< 2.1\%$) because of the scatter effect in high density liquid. These results are consistent with results from a previous study on a conventional linac with 0 T (Martens *et al* 2001, Poppe *et al* 2006, Benítez *et al* 2013, Markovic *et al* 2014, Van Esch *et al* 2014, Stelljes *et al* 2015, International Atomic Energy Agency 2017).

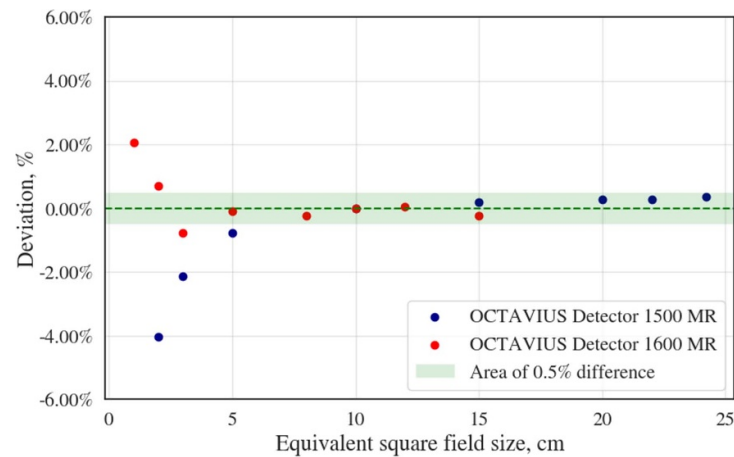


Figure 4. The field size dependence of the OD 1500 MR and OD 1600 MR normalized to the reading of the 10 cm × 10 cm field. The deviations were calculated as percentage differences of each measurement from the ROF calculated in Monaco. Standard deviations were <0.1%. Both systems perform acceptably, but it is noted that the OD 1500 MR tends to underestimate the dose in small fields, whereas the OD 1600 MR overestimates it.

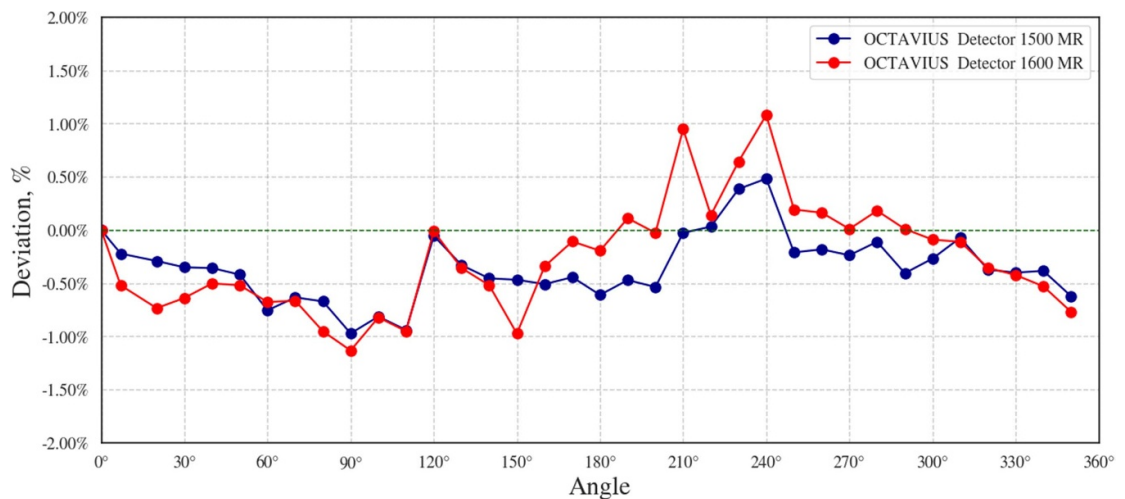


Figure 5. The angular dependence of the OD 1500 MR and OD 1600 MR relative to the Farmer chamber readings, showing acceptable constant sensitivity with standard deviation <0.5%. The data were normalized to 0°.

3.1.4. Angular dependency

OCTAVIUS 4D Phantom MR, maintaining its detector arrays always orthogonal to the radiation beam. Therefore, the angular dependency is expected to be ideal. This expectation is verified for both the OD 1500 MR ($0.2 \pm 0.3\%$) and OD 1600 MR ($0.4 \pm 0.5\%$) (figure 5). The largest deviation is observed when the radiation beam passes through the edge of the couch, where greater dosimetric uncertainty is expected.

3.2. OCTAVIUS Detector 1500 MR in the cylindrical OCTAVIUS 4D Phantom MR

The 25 clinical plans had previously been independently verified with standard gamma criteria. The plans were successfully re-measured and verified using the OCTAVIUS 4D MR and OD 1500 MR. The plans complied with the standard 95% pass rate when applying a 3%/3 mm global gamma criterion, as well as a 90% pass rate when using a 2%/2 mm global gamma criterion and for various targets (figure 6). The average gamma index values ranged from 0.37 to 0.46 for the 3%/3 mm criterion and 0.51 to 0.59 for the 2%/2 mm criterion.

3.3. Measurement with 5 cm lateral phantom offset

Measurements and calculations were performed for one plan with the OCTAVIUS 4D MR centrally located, and with it offset 5 cm laterally to the left. The Gamma comparison was performed, showing similar results for each setup (table 2). This demonstrates that OCTAVIUS 4D Phantom MR measurements can be performed with a lateral offset in order to include an off-axis target.

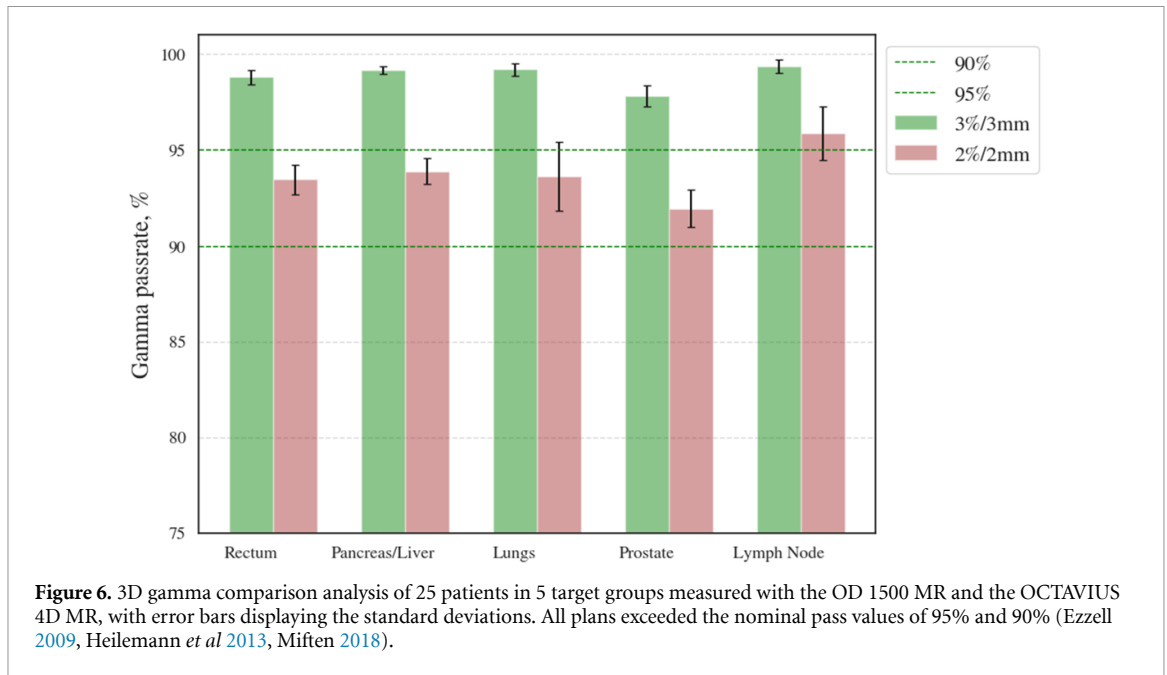


Figure 6. 3D gamma comparison analysis of 25 patients in 5 target groups measured with the OD 1500 MR and the OCTAVIUS 4D MR, with error bars displaying the standard deviations. All plans exceeded the nominal pass values of 95% and 90% (Ezzell 2009, Heilemann et al 2013, Miften 2018).

Table 2. The gamma analysis results for the plan with the standard positioning of the OCTAVIUS 4D Phantom MR and 5 cm left offset. The differences were caused by the strong magnetic field, which varied slightly with lateral position.

	Standard setup		5 cm left offset	
	2%/2 mm	3%/3 mm	2%/2 mm	3%/3 mm
γ	0.522	0.396	0.596	0.453
GPR, %	91.4	99.6	94.6	99.8

Table 3. Average gamma passrate and standard deviations for plans with deliberate position errors across different anatomical sites.

	Rectum		Pancreas/liver		Lungs		Prostate		Lymph nodes	
	2%/2 mm	3%/3 mm	2%/2 mm	3%/3 mm	2%/2 mm	3%/3 mm	2%/2 mm	3%/3 mm	2%/2 mm	3%/3 mm
No error	92.6 ± 1.6	98.8 ± 0.4	94.1 ± 0.4	99.2 ± 0.2	93.6 ± 1.6	99.2 ± 0.3	90.6 ± 1.3	97.8 ± 0.6	92.9 ± 3.5	98.8 ± 1.0
3 mm	88.9 ± 2.1	97.3 ± 0.6	85.0 ± 3.7	96.9 ± 1.2	82.9 ± 3.3	96.6 ± 1.0	82.6 ± 2.0	95.7 ± 1.2	87.0 ± 5.1	97.6 ± 1.7
4 mm	85.3 ± 2.4	95.8 ± 1.0	77.1 ± 4.1	93.4 ± 2.1	73.2 ± 2.1	91.2 ± 1.4	76.0 ± 2.4	92.6 ± 1.9	69.5 ± 2.8	87.8 ± 2.5
5 mm	80.8 ± 2.7	93.4 ± 1.2	69.1 ± 3.4	88.1 ± 2.9	66.9 ± 3.3	86.2 ± 2.9	69.5 ± 2.8	87.8 ± 2.5	69.3 ± 5.5	87.7 ± 6.1

3.4. Position error analysis

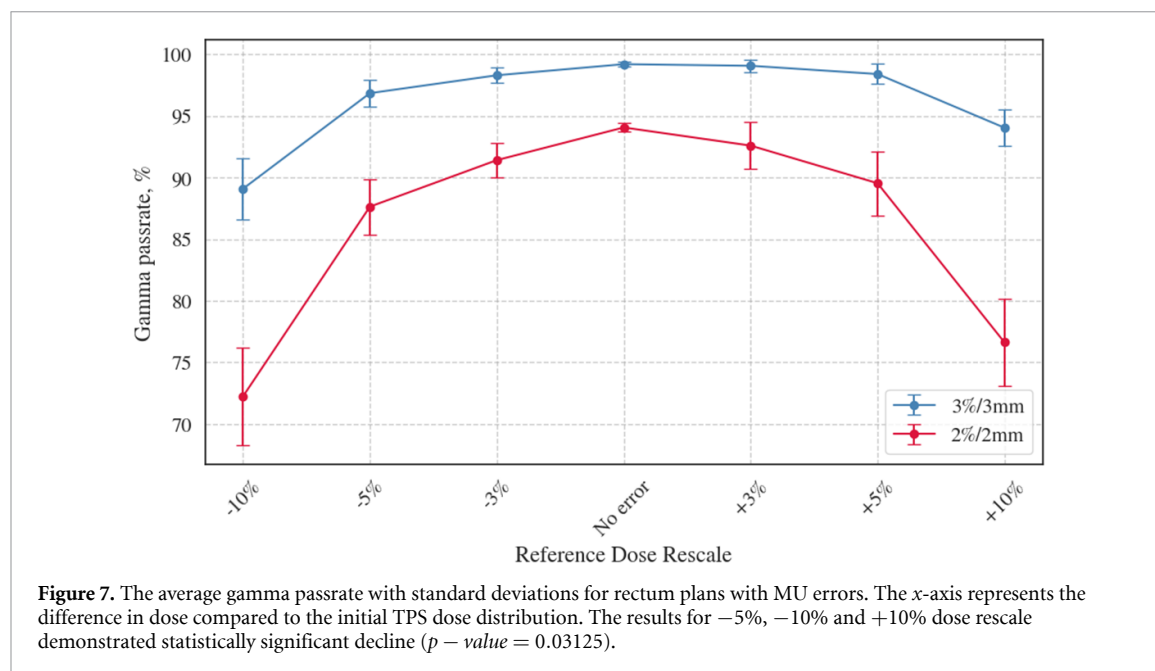
The investigation demonstrated the system’s ability to detect position errors across all treatment plans using the Wilcoxon signed-rank test. As expected, a reduction in gamma passrate was observed in plans where the isocenter shift exceeded the gamma criteria tolerance levels ($p - value = 0.03125$), except for lymph nodes under the 2%/2 mm criterion (table 3). For these plans the Wilcoxon signed-rank test showed a $p - value = 0.09$ for an isocenter shift of 3 mm, and for a minimum detectable error of 4 mm test demonstrated a $p - value = 0.03125$.

3.5. MU errors detection

The results of the gamma analysis are shown in table 4. The system is not sensitive to small dose errors when using 3%/3 mm and 2%/2 mm criteria with a 10% low-dose threshold. The one-tailed Wilcoxon signed-rank test revealed a statistically significant decline for plans with 5% overdose and 10% underdose ($p - value < 0.032$). Within these settings, larger targets, such as the rectum and prostate, showed greater sensitivity to dose changes than smaller targets (figure 7). The results also indicated that OD 1500 MR was more sensitive in detecting errors caused by overdose than underdose. This increased sensitivity is due to the gamma pass rate equation, where the dose difference is normalized to the point receiving the highest dose (equation (5) in Low et al (1998)). Consequently, when underdose occurs, the relative dose difference is smaller, allowing more background points to pass the criteria.

Table 4. Average gamma passrate and standard deviations for plans with deliberate MU errors across different anatomical sites. The scaling was performed within the TPS. Therefore positive scaling indicates measurement ‘underdose’ and negative scaling indicates measurement ‘overdose’.

MU error	Rectum		Pancreas/liver		Lungs		Prostate		Lymph nodes	
	2%/2 mm	3%/3 mm	2%/2 mm	3%/3 mm	2%/2 mm	3%/3 mm	2%/2 mm	3%/3 mm	2%/2 mm	3%/3 mm
+10%	52.1 ± 6.8	72.0 ± 5.9	76.6 ± 3.6	94.0 ± 1.5	73.8 ± 6.1	92.8 ± 2.9	97.1 ± 0.6	71.4 ± 2.7	78.7 ± 5.7	95.0 ± 2.5
+5%	76.3 ± 5.9	90.1 ± 4.3	89.5 ± 2.6	98.4 ± 0.8	90.1 ± 0.7	98.7 ± 0.2	88.0 ± 1.9	97.1 ± 0.6	90.3 ± 4.3	98.5 ± 0.9
+3%	87.0 ± 4.1	96.8 ± 1.3	92.6 ± 1.9	99.1 ± 0.5	93.5 ± 0.9	99.4 ± 0.2	92.1 ± 1.2	98.8 ± 0.2	92.5 ± 3.9	99.0 ± 0.8
No error	92.6 ± 1.6	98.8 ± 0.4	94.1 ± 0.4	99.2 ± 0.2	93.6 ± 1.6	99.2 ± 0.3	90.6 ± 1.3	97.8 ± 0.6	92.8 ± 3.5	98.8 ± 1.0
-3%	79.5 ± 1.8	91.4 ± 1.8	91.4 ± 1.4	98.3 ± 0.6	88.4 ± 2.6	97.2 ± 1.4	79.7 ± 3.6	92.1 ± 2.0	89.2 ± 4.0	97.6 ± 1.3
-5%	70.3 ± 2.5	83.2 ± 1.6	87.6 ± 2.3	96.8 ± 1.1	82.4 ± 3.9	94.5 ± 2.4	71.4 ± 4.0	85.7 ± 3.3	84.6 ± 5.5	95.7 ± 2.0
-10%	50.0 ± 3.0	66.1 ± 2.7	72.3 ± 4.0	89.1 ± 2.5	62.9 ± 7.0	82.4 ± 6.1	54.1 ± 3.0	68.6 ± 4.4	69.0 ± 8.2	86.2 ± 6.3



4. Conclusion

The new MR-compatible OCTAVIUS detectors have shown acceptable results in the basic dosimetry tests within a 1.5 T magnetic field. Good QA performance has been demonstrated with OCTAVIUS Detector 1500 MR and the OCTAVIUS 4D Phantom MR in a 1.5 T MR-linac. The system has also shown its capability to perform measurements with the lateral offset position. OCTAVIUS Detector 1500 MR with OCTAVIUS 4D Phantom MR can successfully differentiate between standard plans and plans with position errors. However, it is noted that the gamma test is not optimal for detecting dose differences in highly modulated beams. While large differences in dose can be observed, for small dose differences an additional measure such as evaluation of mean dose or reference point dose increases the effectiveness of the QA system.

Data availability statement

All data that support the findings of this study are included within the article (and any supplementary information files).

Acknowledgments

This work was supported by the ADEQUATE project [Dutch Science Organization (NWO) Applied Sciences]. The authors would also like to thank PTW for temporarily providing the OCTAVIUS 4D MR system with OD 1500 MR and OD 1600 MR arrays.

ORCID iD

Viktoriia Gorobets  <https://orcid.org/0009-0002-3265-8176>

References

- Benítez E, Casado F, García-Pareja S, Martín-Viera J, Moreno C and Parra V 2013 Evaluation of a liquid ionization chamber for relative dosimetry in small and large fields of radiotherapy photon beams *Radiat. Meas.* **58** 79–86
- Brand N, Albrecht C and Loutfi-Krauß B 2022 Quality assurance with OCTAVIUS detector 1600 SRS at the CyberKnife (available at: www.ptwdosimetry.com)
- Ezzell G A et al 2009 TG-119 IMRT commissioning tests instructions for planning, measurement and analysis *Med. Phys.* **36** 5359–73
- Ezzell G A, Galvin J M, Low D, Palta J R, Rosen I, Sharpe M B, Xia P, Xiao Y, Xing L and Yu C X 2003 Guidance document on delivery, treatment planning and clinical implementation of IMRT: report of the IMRT subcommittee of the AAPM radiation therapy committee *Med. Phys.* **30** 2089–115
- Heilemann G, Poppe B and Laub W 2013 On the sensitivity of common gamma-index evaluation methods to MLC misalignments in Rapidarc quality assurance *Med. Phys.* **40** 031702
- Houweling A, De Vries J, Wolthaus J, Woodings S, Kok J, Van Asselen B, Smit K, Bel A, Lagendijk J and Raaymakers B 2016 Performance of a cylindrical diode array for use in a 1.5 T MR-linac *Phys. Med. Biol.* **61** N80
- International Atomic Energy Agency 2017 *Dosimetry of Small Static Fields Used in External Beam Radiotherapy (Technical Reports Series vol 483)* (International Atomic Energy Agency)
- Knill C, Snyder M, Rakowski J T, Zhuang L, Matuszak M and Burmeister J 2016 Investigating ion recombination effects in a liquid-filled ionization chamber array used for IMRT QA measurements *Med. Phys.* **43** 2476–84
- Lagendijk J J, Raaymakers B W and Van Vulpen M 2014 The magnetic resonance imaging–linac system *Seminars in Radiation Oncology* vol 24 (Elsevier) pp 207–9
- Laub W U and Wong T 2003 The volume effect of detectors in the dosimetry of small fields used in IMRT *Med. Phys.* **30** 341–7
- Low D A, Harms W B, Mutic S and Purdy J A 1998 A technique for the quantitative evaluation of dose distributions *Med. Phys.* **25** 656–61
- Markovic M, Stathakis S, Mavroidis P, Jurkovic I-A and Papanikolaou N 2014 Characterization of a two-dimensional liquid-filled ion chamber detector array used for verification of the treatments in radiotherapy *Med. Phys.* **41** 051704
- Martens C, De Wagter C and De Neve W 2001 The value of the LA48 linear ion chamber array for characterization of intensity-modulated beams *Phys. Med. Biol.* **46** 1131
- Miften M et al 2018 Tolerance limits and methodologies for IMRT measurement-based verification QA: *Recommendations of AAPM Task Group No. 218* *Med. Phys.* **45** e53–e83
- Mönnich D, Winter J, Nachbar M, Künzel L, Boeke S, Gani C, Dohm O, Zips D and Thorwarth D 2020 Quality assurance of IMRT treatment plans for a 1.5 T MR-linac using a 2D ionization chamber array and a static solid phantom *Phys. Med. Biol.* **65** 16NT01
- Olaciregui-Ruiz I, Vivas-Maiques B, Kaas J, Perik T, Wittkamper F, Mijnheer B and Mans A 2019 Transit and non-transit 3D EPID dosimetry versus detector arrays for patient specific QA *J. Appl. Clin. Med. Phys.* **20** 79–90
- Pappas E, Maris T, Papadakis A, Zacharopoulou F, Damilakis J, Papanikolaou N and Gourtsoyiannis N 2006 Experimental determination of the effect of detector size on profile measurements in narrow photon beams *Med. Phys.* **33** 3700–10
- Pardo-Montero J and Gómez F 2009 Determining charge collection efficiency in parallel-plate liquid ionization chambers *Phys. Med. Biol.* **54** 3677
- Poppe B, Blechschmidt A, Djouguela A, Kollhoff R, Rubach A, Willborn K C and Harder D 2006 Two-dimensional ionization chamber arrays for IMRT plan verification *Med. Phys.* **33** 1005–15
- Poppinga D, Schrenk O, Renkamp K and Klüter S 2021 OCTAVIUS® based plan verification at a MRIdian® linac (available at: www.ptwdosimetry.com)
- Roberts D A et al 2021 Machine QA for the Elekta Unity system: a report from the Elekta MR-linac consortium *Med. Phys.* **48** e67–e85
- Stelljes T S, Harmeyer A, Reuter J, Looe H K, Chofor N, Harder D and Poppe B 2015 Dosimetric characteristics of the novel 2D ionization chamber array OCTAVIUS Detector 1500 *Med. Phys.* **42** 1528–37
- Takei H, Isobe T, Kitamura N, Mori Y, Tomita T, Kobayashi D, Kamizawa S, Sato T, Sakurai H and Sakae T 2018 General ion recombination effect in a liquid ionization chamber in high-dose-rate pulsed photon and electron beams *J. Radiat. Res.* **59** 282–5
- Van Esch A, Basta K, Evrard M, Ghislain M, Sergent F and Huyskens D P 2014 The OCTAVIUS1500 2D ion chamber array and its associated phantoms: dosimetric characterization of a new prototype *Med. Phys.* **41** 091708